Predissociation of the Hydroxymethyl Radical in the $3p_z$ Rydberg State: Formaldehyde + Hydrogen Atom Channel†

D. Conroy, V. Aristov, L. Feng, and H. Reisler*

Department of Chemistry, University of Southern California, Los Angeles, California 90089-0482

Received: April 7, 2000; In Final Form: June 19, 2000

The photodissociation of the hydroxymethyl radical to hydrogen atom and formaldehyde was investigated following excitation to the origin band of the Rydberg $^2A''(3p_z)$ state of jet cooled CH_2OD and CD_2OH. D and H products were detected by 2-color laser ionization. The peaks in the photofragment yield spectrum of the D product from CH_2OD correspond to peaks in the absorption spectrum, and this establishes hydroxymethyl as the source of the observed D atoms. D atoms appear as major products from CH_2OD, but the H photofragment yield is not discernible above the background. On the other hand, in the dissociation of CD_2-OH, only H atoms are produced. It is concluded that isomerization to the methoxy radical is not important. Time-of-flight distributions of the D atom from CH_2OD were obtained under core sampling conditions. The product translational energy distribution derived from the data is broad, indicating that the formaldehyde cofragment is produced in the ground electronic state but with an internal energy distribution that extends to the thermochemical limit. The recoil anisotropy parameter was estimated by comparing the intensity of the D signals obtained with parallel and perpendicular polarization of the photolysis laser. The observed anisotropic angular distribution suggests that the dissociation is fast, as also indicated by the line width. The results can be rationalized by a mechanism that involves nonadiabatic transitions from the initially excited Rydberg state to the ground state, with the final crossing occurring in a region of the potential energy surface that leads to direct O−D(H) fission without isomerization. Exit channel dynamics is probably responsible for the high vibrational excitation of the formaldehyde fragment.

1. Introduction

The hydroxymethyl radical (CH_2OH) and its isomer, the methoxy radical (CH_3O) are important species in fuel combustion and in atmospheric and interstellar chemistry. CH_2OH, being much more reactive than CH_3O, is also of importance in polluted environments.[1] The isomerization $CH_2OH \leftrightarrow CH_3O$ is intriguing because the calculated barrier is comparable to the $H + CH_2O$ dissociation barrier.[2,3] However, despite considerable theoretical interest in this system, experimental studies of the uni- and bimolecular reactions of CH_2OH are sparse, due mainly to difficulties in preparing this reactive species.[4,5]

Recently, we have succeeded in producing the radical in a molecular beam using the photoinitiated reaction $Cl + CH_3OH \rightarrow HCl + CH_2OH$. The reaction is carried out in a quartz tube extension to the pulsed valve under conditions that suppress the rapid consecutive reaction $Cl + CH_2OH \rightarrow CH_2O + HCl$.[4]

Using this method for production of the radical and resonance enhanced multiphoton ionization (REMPI) for its detection,[1,6,7] we obtained rotational envelopes of selected vibronic bands following excitation to the 3*p* Rydberg state, whose origin lies at ∼243 nm.[1] Analysis of the rotational contours led to assignment of the 3*p* Rydberg state as $^2A''(3p_z)$.[4] The 11 cm^{-1} homogeneous line width inferred from the spectral simulations implies that the upper state is predissociative, although no dissociation products have been observed.

In this paper, we report the first results identifying H(D) as a photodissociation product of $CH_2OH(D)$ following excitation in the origin band of the $^2A''(3p_z) \leftarrow {}^2A''(\pi^*)$ transition. Because of the large H background in our apparatus, the isotopes CH_2-OD and CD_2OH were used. The D photofragment was examined using the "core sampling" variant of time-of-flight (TOF) spectroscopy. Both the kinetic energy release and the effective recoil anisotropy parameter, β_{eff}, were determined.

The study of the photodissociation dynamics on the $^2A''(3p_z)$ surface is intriguing for several reasons. First, excitation accesses a vibronically resolved Rydberg state, and therefore Rydberg−valence interaction must influence the subsequent dynamics. Second, there is more than one pathway that can terminate in D photofragments. Third, the role of isomerization to the methoxy radical can be investigated by comparing the H and D signals obtained in the photolysis of CD_2OH and CH_2OD. We note that in the photodissociation of CH_3O from the first excited $^2A_1$ state, the $CH_2 + OH$ channel, which involves isomerization, has been observed.[8,9] Fourth, there are additional distinct chemical channels that are energetically accessible from the $^2A''(3p_z)$ state, e.g., $CH_2 + OH$, $H_2 + HCO$ etc., but have not yet been observed. Last, the combination of a structured vibronic spectrum and multiple dissociation pathways opens the possibility of observing mode or bond specificity in the dissociation. In this paper we discuss in detail the D product obtained following excitation to the origin band.

2. Experimental Section

2.1. Production and Detection of CH_2OD and CD_2OH. The experimental apparatus utilized in the production and subsequent studies of hydroxymethyl radical molecular beams has been described in a previous publication.[4] A brief summary emphasizing subsequent improvements is presented here.

Reactant mixtures of Cl_2, CH_3OD, or CD_3OH (Aldrich, used without further purification) and He are prepared in a glass and Teflon gas delivery line. First, methanol is allowed to evaporate (∼100 Torr) into a 5.0 L glass reservoir. Next, a 5% Cl_2/He

† Part of the special issue "C. Bradley Moore Festschrift".

* Corresponding Author. E-mail: reisler@chem1.usc.edu

10.1021/jp001357s CCC: $19.00
Published on Web 07/28/2000

mixture is added in an amount adjusted to achieve a final 1−2% Cl_2 concentration. Last, helium is added to a total pressure of 3 atm, and the mixture is introduced into the vacuum chamber via a nonmetal piezoelectrically driven pulsed nozzle[10] (∼250 μs fwhm**)** through a ∼4 mm long quartz tube (∼1 mm i.d.) affixed to the faceplate with sodium silicate adhesive. Photodissociation of Cl_2 is achieved with the tripled output of a Nd:YAG laser (Quanta-Ray DCR-1, 355 nm, 8 mJ) directed onto the quartz tube. The hydroxymethyl radical temperature is estimated from rotational band contour simulations at 10 K.[4]

The vacuum apparatus consists of two differentially pumped chambers: a source chamber containing the nozzle, and a detection chamber containing the TOF mass spectrometer, both evacuated by turbomolecular pumps. The source and detection chambers are joined by a flange on which a skimmer is mounted. The effluent of the nozzle is skimmed (Beam Dynamics, 1.51 mm dia.) at a distance of ∼10 mm from the quartz tube and passes into the detection region. The pressure in the detection region is $\sim 1 \times 10^{-7}$ Torr with the nozzle operating at 10 Hz, while the base pressure is $\sim 4 \times 10^{-9}$ Torr.

Isotopomers of CH_2OH are detected with a combination of REMPI spectroscopy and TOF mass spectrometry using published assignments.[1] Rydberg excitation and REMPI of the hydroxymethyl radical is achieved using the focused, linearly polarized output of an excimer- or YAG-pumped dye laser system (Lambda-Physik EMG201/LPD3000 or Continuum NY81C/ND6000, Coumarin 440, 450, 460, 480). The REMPI spectra confirm the isotopic purities of CH_2OD and CD_2OH.

In the visible 1-color (2+1) REMPI detection of the hydroxymethyl radical, absorption of two focused, 440−490 nm photons (2 mJ, 30 cm f.l. lens) excites the radical resonantly to the $3p_z$ Rydberg state, while a third photon of the same wavelength ionizes the excited molecule. In the UV 1-color (1+1) REMPI scheme, Rydberg excitation is accomplished with one 220−245 nm photon (200 μJ, 50 cm f.l. lens), with subsequent ionization by another photon.

2.2. Detection of D atoms. H(D) atoms are detected via 2-color (1+1) REMPI. Absorption of a photon at 121.6 nm excites the Lyman-α transition, and is followed by ionization with a 365 nm photon. The doubled output (365 nm, 2 mJ) of a YAG-pumped dye laser system (Continuum PL8010/ND6000, LDS751) is focused (20 cm f.l. lens) into a mixture of Kr (75 Torr) and Ar (310 Torr).[11] The tripled 121.6 nm light is then introduced into the REMPI detection region (75 mm f.l. MgF_2 lens), along with the residual 365 nm light.

Ions are accelerated (265.5 V or 2.5 kV) toward a 1 in. dia. multichannel plate (MCP) detector (Galileo, 25 mm) through a Wiley−McLaren TOF mass spectrometer,[12] which is mounted vertically. For core sampling, the two-stage ion acceleration region is maintained at electrical field strengths of 69 V cm^{-1} and 231 V cm^{-1}, which corresponds to the spatial focusing condition for the geometry of the apparatus. The MCP output is amplified, digitized, and transferred to a dedicated software package that averages the signals (typically, 10 to 10 000 laser shots) and records portions of the TOF trace. Time delays are controlled with delay generators, and the dye laser grating steps are controlled by the computer. Laser wavelengths are calibrated using known frequencies of H, D, and CH_2OH(D) REMPI lines.[1,13,14]

2.3. Core sampling. The core sampling technique utilizes a spatial restriction in the ion detection in order to eliminate contributions from off-axis ions, thereby yielding the speed distribution of the recoiling fragments in a straightforward manner. This allows the measurement of differential cross-sections as a function of kinetic energy and the angle between the recoil and the photolysis laser polarization directions.[15,16]

The differential cross-section of a photodissociation event leading to two photofragments, assuming an isotropic distribution of the transition dipole moment (ensemble of unaligned molecules), is a probability function expressed (in terms of kinetic energy T and recoil angle θ with respect to the photolysis laser polarization vector) by

$$\sigma_\theta(T) = \frac{d^2\sigma}{dT\, d\Omega} = \frac{N}{4\pi} P(T)\{1 + \beta P_2(\cos\theta)\} \qquad (1)$$

where $d\Omega$ is the differential solid angle $\sin\theta\, d\phi\, d\theta$, N is the number of dissociating parent molecules, $P(T)$ is the kinetic energy distribution of photofragments, β is the anisotropy parameter, and $P_2(\cos\theta)$ is the second Legendre polynomial of the cosine of θ. The limiting values of β for fast dissociation and axial recoil are -1 for recoil perpendicular ($\perp$) to the transition dipole moment (μ_e), and 2 for the parallel case ($\parallel$)

In practice, the finite diameter of the aperture allows detection of ions slightly off the TOF axis, which is expressed as a distribution in energy space by,[15]

$$I_\theta(T_z) = k_I \int_{T_z}^{T_a} P(T)\{1 + \beta P_2(\cos\theta)\}\, dT \qquad (2)$$

where T_z is the kinetic energy of particles aligned directly along the TOF axis and T_a is the kinetic energy of particles which just miss the edge of the aperture. $T_a \equiv T_z + 1/2m\,(r/t)^2$, where r is the aperture radius and t is the arrival time. The normalization constant, k_I, can be determined by measuring the total cross section and is neglected in this work.

The effective anisotropy parameter, β_{eff}, as a function of photofragment product kinetic energy is derived from measurements of the product intensity at parallel and perpendicular polarizations of the photolysis laser with respect to the TOF axis. It is given by[15]

$$\beta_{eff}(T_z) = 2\frac{I_\parallel(T_z) - I_\perp(T_z)}{I_\parallel(T_z) + 2I_\perp(T_z)} \qquad (3)$$

where $I(T_z)$ is the measured distribution in kinetic energy space. The data are then scaled using $\beta_{eff}(T_z)$ and summed to produce the total kinetic energy distribution of the photofragments, irrespective of the anisotropy. This is done by solving eq 2 for $P(T)$ with the approximation $P(T_z) \approx P(T_a)$,[15] then combining the results from the two different polarizations.

In the current application, a metal plate with a 4 mm dia. hole is positioned in front of the MCP detector to prevent detection of ions (whose average TOF is ∼1.4 μs) with a sizable velocity component perpendicular to the TOF axis. This aperture is mounted on a linear motion feedthrough (MDC, BLM-133-4) to allow alternation between total ion collection and core sampling. The photodissociation laser polarization is rotated in a way that minimizes changes in laser alignment and power. In the core-sampling application, the photolysis laser is loosely collimated with a 1 m f.l. lens in order to minimize ionization and facilitate alignment.

The transformations of the measured TOF traces $I(t_z)$ into velocity $I(v_z)$ or kinetic energy $I(T_z)$ space are performed using appropriate Jacobians under space focusing conditions. Here, we use the approximation $v_z \approx A_S\,(t - t_0)$, where A_S is the acceleration experienced by the detected particle due to the static field of the ion source and $(t - t_0)$ is the difference in arrival times of the particles relative to the center of the distribution.[15]

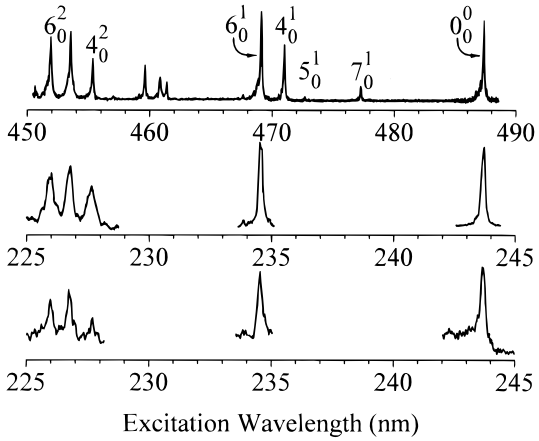

Figure 1. Visible (2+1) REMPI spectrum of CH_2OD (upper panel) with assignments from ref 1. The middle panel shows portions of the same spectrum obtained by UV (1+1) REMPI, while the bottom panel shows the D atom (2+1) REMPI signal obtained under the same excitation conditions.

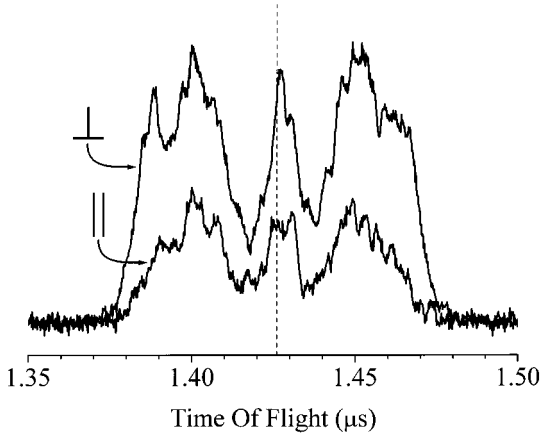

Figure 2. TOF spectra of D photofragments obtained from CH_2OD under core sampling conditions. The traces obtained with parallel and perpendicular polarizations of the excitation laser are shown after background subtraction. The center of the distribution is marked by a dashed line. 5000 laser firings are summed for each trace.

Since this is the first report of results from our core sampling TOF spectrometer, the time profiles and energy distributions obtained in the 121.6 nm photodissociation of acetylene were used to test our operating procedures.[16]

3. Results

3.1. Photofragment Yield Spectra of D Atoms from CH_2OD and CD_2OH. Because other sources in the reactive mixture may give rise to a D atom signal, it is imperative to establish a direct correspondence between the absorption features of CH_2OD and the observed D signal. For this reason, photofragment yield spectroscopy was carried out in selected regions of the absorption spectrum of CH_2OD. The top panel of Figure 1 presents a (2+1) REMPI spectrum of jet-cooled CH_2OD radical. Nonsaturated conditions are verified by observing the spectral intensities and bandwidths as a function of excitation laser energies. The vibrational assignment of the (2+1) spectrum was taken from Johnson and Hudgens.[1]

The middle panel displays a (1+1) REMPI spectrum of the bands chosen for the photofragment yield study. Bands that overlap with DCl (2+1) REMPI lines and lead to D production were excluded. The bottom panel shows the photofragment yield spectrum, namely, the variation of the D atom (1+1) REMPI signal obtained as the pump laser is scanned through the chosen CH_2OD vibronic bands. The clear correspondence between the D and CH_2OD spectral features indicates that deuterium is a product of the dissociation of the excited hydroxymethyl radical. The cofragment is most likely formaldehyde, as discussed below. In contrast, no H atom signal corresponding to the absorption features of CH_2OD was observed. Since the H atom background in our apparatus is larger than the D atom background, we also searched for D atom signal from CD_2OH. This signal was very small, whereas the H signal was large, indicating that it is the O−H(D) bond that preferentially breaks (see below). We note that the bandwidths of the origin bands in CH_2OD and CD_2OH are comparable, indicating that the predissociation time scales are similar.

3.2. Kinetic Energy Distributions of Nascent D Atoms. Figure 2 shows background subtracted TOF spectra of D atoms obtained in the core sampling mode following excitation of the origin band with laser polarizations parallel and perpendicular to the ion flight axis. The pump laser was tuned to the peak in the origin band, while the probe was set at the center of the Doppler profile of the D photofragment. For each TOF spectrum

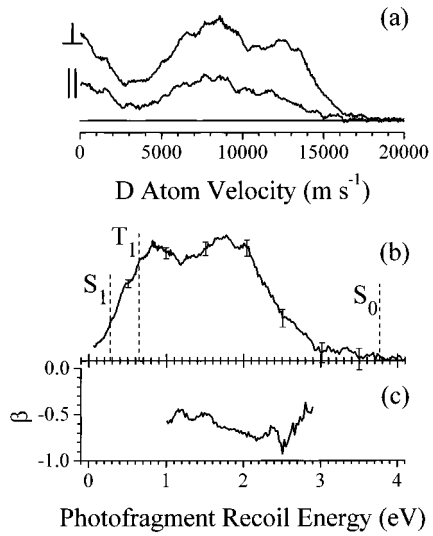

Figure 3. (a) D photofragment speed distributions obtained with parallel and perpendicular polarizations of the excitation laser from TOF traces such as the one shown in Figure 2. The relative intensities are used to derive the β parameter shown in part (c). The region of small recoil, where the core sampling assumption breaks down, is excluded. (b) The total translational energy distribution of the recoiling fragments obtained by transformation of the data in part (a) and scaling according to β_{eff} (see the text for details). The maximum translational energies allowed for channels I(a−c) are shown with dashed lines. (c) The effective recoil anisotropy parameter β_{eff} obtained from part (a) plotted as a function of translational energy.

several ON/OFF experiments were carried out by monitoring the D signals with either the probe, pump, or 355 nm radiation blocked. The largest background signal was obtained with the 355 nm radiation OFF but all other lasers ON, and is concentrated in the region near the center of the TOF distribution (small recoil). We note that in the region of small recoil ($4 \times v < r/t$), the core-sampling assumption breaks down.[15] This leads to a large increase in the collection efficiency, and an enhancement of the signal intensity compared to the signal observed in the region where the core sampling assumption is obeyed. This region is excluded in the analysis.

In Figure 3a the corresponding velocity distribution is shown, and the distribution of *total* translational energy of photofragments is depicted in Figure 3b, which also indicates the kinetic energy limits associated with production of the formaldehyde cofragment in the electronic states $S_0(^1A_1)$, $T_1(^3A_1)$, and S_1-

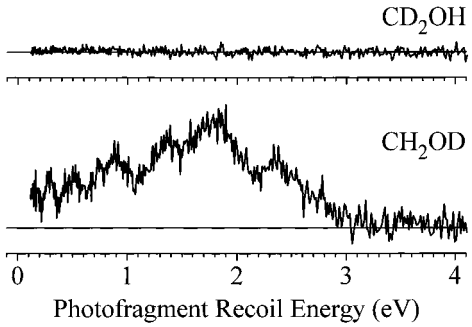

Figure 4. Comparison of the D atom signal as a function of translational energy obtained in the dissociation of CD_2OH (upper panel, 20 000 laser firings) and CH_2OD (lower panel, 10 000 laser firings) after background subtraction. This experiment, carried out with the core sampling aperture removed, shows that the D signal from CD_2OH is negligible.

($^1A_2$). Clearly, the large fraction of D atoms with high kinetic energies identifies the ground-state of formaldehyde as the dominant cofragment. The energetic limit for production of ground-state D + CH_2O fragments is ~3.8 eV, and thus we conclude that formaldehyde is formed with considerable internal excitation. The excitation peaks at ~1−2 eV, exhibiting a broad, structureless distribution that decreases gradually beyond the maximum.

Despite the large amount of internal excitation seen in the formaldehyde fragment, there is no perceptible evidence for isomerization of the parent. This has already been implied by the results described above. As additional confirmation, Figure4 compares the kinetic energy distributions of D photofragments obtained from CH_2OD and CD_2OH. The core-sampling aperture was removed in this experiment in order to improve sensitivity, because our goal here was to compare the total signals. Integrations of the distributions show that the D atom signal from CH_2OD is more than 40-fold larger than that from CD_2OH. When the isotope abundance is considered, this measurement indicates that the fraction of D atoms produced via the methoxy route is insignificant.

3.3. D Atom Angular Distributions from CH_2OD. The angular distribution of the products was inferred from measurements carried out at parallel and perpendicular polarizations of the photolysis laser with respect to the TOF axis (Figure 3a). Assuming that the detection efficiency is constant and that the alignment has not been changed as a result of rotation of the laser polarization, the anisotropy parameter is determined as a function of total kinetic energy using eq 3. The result is given in Figure 3c. Since we find that contaminations sometimes affect the D signal at low kinetic energies, we show results only at $T \geq 1$ eV. The derived average anisotropy parameter is $\beta_{\text{eff}} = -0.6 \pm 0.3$.

Several factors can lead to an observed anisotropy that differs from the limiting cases, even when the dissociation is much faster than the rotational period. One of these factors is the angle of the breaking bond relative to the direction of the transition dipole moment. For triatomic and larger molecules, deviations from the limiting values of 2 and −1 (for parallel and perpendicular transitions, respectively) occur when the breaking bond angle is neither parallel nor perpendicular to the direction of the transition dipole moment, μ_e. In CH_2OH, the C−O−H angles were computed ab initio to be 108.4 ° and 115.1° for the ground and excited state, respectively,[1] while μ_e was found to be collinear with the C−O bond.[4] For axial recoil along the O−H (or O−D) bond, the expected anisotropy, $\beta_\chi \equiv 2P_2(\cos\chi)$,[17] is −0.46 to −0.70, corresponding to the ground-state and excited-state geometries of CH_2OD (assuming that they do not change for the different isotopomers). The surface crossings that are required to reach the D + $CH_2O(S_0)$ channel (see below) may further modify this angle. The observed value of β_{eff} is within the expected range and indicates a fast dissociation process.

4. Discussion

In discussing the photoinitiated decomposition of CH_2OH from the $3p_z$ Rydberg state, two aspects must be considered. First, radicals have typically low dissociation thresholds and can often couple to several dissociation continua simultaneously. Second, excited Rydberg states usually correlate with excited states of the products, and thus nonadiabatic surface crossings should dominate the dynamics.

The hydroxymethyl radical is no exception, and in addition it provides an opportunity to assess the participation of the $CH_2OH \leftrightarrow CH_3O$ isomerization in the dissociation. The D photofragment of CH_2OD reported in this paper can be generated via several pathways, some of which give rise to concomitant production of H atoms. The most likely channels and their thermochemical thresholds (evaluated for the appropriate isotopomer) are given below:[1,18−22]

$$CH_2OD \rightarrow CH_2O\,(S_0) + D \quad \Delta H = 1.32 \pm 0.07 \text{ eV} \qquad \text{(Ia)}$$

$$\rightarrow CH_2O\,(T_1) + D \quad \Delta H = 4.44 \pm 0.07 \text{ eV} \qquad \text{(Ib)}$$

$$\rightarrow CH_2O\,(S_1) + D \quad \Delta H = 4.81 \pm 0.07 \text{ eV} \qquad \text{(Ic)}$$

$$CH_2OD \rightarrow HCOD + H \quad \Delta H \approx 3.54 \text{ eV} \qquad \text{(II)}$$

$$CH_2OD \rightarrow H_2 + CO + D \quad \Delta H = 1.31 \pm 0.02 \text{ eV} \qquad \text{(IIIa)}$$

$$\rightarrow HD + CO + H \quad \Delta H = 1.28 \pm 0.02 \text{ eV} \qquad \text{(IIIb)}$$

$$CH_2OD \leftrightarrow CH_2DO \rightarrow CH_2O + D \quad \Delta H = 1.32 \pm 0.07 \text{ eV} \qquad \text{(IVa)}$$

$$\rightarrow CHDO + H \qquad \text{(IVb)}$$

Excitation deposits 5.08 eV (40 950 cm^{-1}) in CH_2OD, making all of these channels energetically accessible.

As inferred from the comparison between the D and H atom signal intensities obtained in the dissociation of $CH_2OD(3p_z)$ and $CD_2OH(3p_z)$ in their ground vibrational states, the isomerization channel (IV) is not important. The large fraction of D fragments with translational energies exceeding 1 eV indicates that channel Ia must be a major pathway. Small contributions from channels Ib and Ic, however, cannot be precluded. The negligible D signal from CD_2OH also rules out channel II as a major pathway. To assess the importance of channel III, we searched for CO(v=0) signal using (2+1) REMPI via the B state at 230.1 nm. No signal was observed, despite the high detection sensitivity for this transition.[23] However, the appearance of CO in higher vibrational states cannot be excluded.

Having established that the terminus of dissociation leading to D photofragments via the $3p_z$ Rydberg state is predominantly channel Ia, the next step is to examine the nonradiative pathways that can lead to its formation. The potential energy surface of ground-state hydroxymethyl radical has a barrier in the channel leading to H + $CH_2O(S_0)$ estimated theoretically at ~2 eV.[2,3] The ground-state radical is nonplanar and thus belongs to the C_1 symmetry point group.[1] Distortion from planarity reduces the electron occupation of the π^*_{CO}(a") HOMO, thereby enhancing the stability of the radical.[6] However, because the radical has finite energy barriers in the CH_2 wag coordinate (which is mixed with the torsion), the equivalent structures

rapidly interconvert, and the ground-state electronic wave function complies with C_s A" symmetry.[1] A state of A" symmetry does not correlate with the $CH_2O(^1A_1) + D(^1S)$ channel, which has A′ symmetry, and this may account for the barrier in the dissociation to channel Ia.[2,3]

According to ab initio calculations, three other Rydberg states lie below the $3p_z$ state ($3p_y$, $3p_x$, and $3s$).[24] All have geometries similar to that of ground-state CH_2OH^+; i.e., planar (C_s symmetry) with a C−O bond length similar to that of the double bond (1.243 Å as compared with 1.3626 Å for the ground state).[1] These states are located at energies lower than the $3p_z$ state by up to 1.2 eV. The absorption spectrum, which shows structured features below the $3p_z$ origin,[24] confirms the existence of bound states with energies in the Franck−Condon region as low as 4.3 eV above the ground state.

Pathways Ib and Ic, which yield formaldehyde in its valence (n,π^*) singlet and triplet states (A_2 symmetry), correlate in C_s symmetry with A" excited states. However, if these channels are to correlate with the $3p_z$(A") state, Rydberg−valence configuration mixing must occur. Product channels in which formaldehyde is formed in the 3*s* and 3*p* Rydberg states do correlate with the 3*s* and 3*p* Rydberg states of hydroxymethyl, but their thermochemical thresholds are at ∼8.4 and 9.3 eV, respectively, much higher than the origin of the $3p_z$ state of CH_2OD (5.1 eV).[1,20]

Because of the proximity of the $3p_z$ state to the other Rydberg states, Franck−Condon considerations would favor initial couplings to one or more of these states, leading to a sequential coupling mechanism finally terminating in a crossing to the ground state and channel Ia products. Calculations taking into account only valence states indicate that most of the excited states are repulsive.[25] No calculations including both valence and Rydberg states have yet been reported; thus, the issue of the specific nonadiabatic interactions leading to channel Ia remains open.

The existence of clear vibronic structure in the $^2A''(3p_z) \leftarrow {}^2A''(\pi^*)$ transition with an inferred homogeneous linewidth of $\sim 10\ cm^{-1}$ (similar in the origin bands of all the isotopomers) indicates that the excited radical decays from its initial state in ≤ 1 ps. Combined with the anisotropy observed in the fragment angular distribution, it leads to the conclusion that the dissociation lifetime is of comparable duration; i.e., on the order of a picosecond.

The short time scale for dissociation is the clue to understanding the seemingly contradictory observations of a broad internal energy distribution in the formaldehyde product, which is nevertheless accompanied by no isotope scrambling in the products (no isomerization). The shape of the internal energy distribution is similar to that which is expected from a statistical-like dissociation, in which case the energy would be fully randomized in the activated complex. Because the excitation energy (5.1 eV) is much greater than the barrier to isomerization (1.8 eV),[2,3] such a mechanism would imply a significant probability for isomerization during the dissociation. The absence of isomerization suggests therefore that the high internal excitation of the formaldehyde fragment derives from dynamical biases in the exit channel for O−D(H) fission. In the absence of calculations of potential energy surfaces and crossing seams for the nonadiabatic transitions, it is unwarranted to speculate further on the dynamics. It is noteworthy, however, that a comparably high degree of fragment internal excitation has been observed previously in another H atom fission reaction initiated by photoexcitation of a Rydberg state. In the 121.6 nm dissociation of acetylene, the maximum allowed kinetic energy release is ∼4.5 eV, but the peak in the translational energy distribution is around 1 eV, implying that the C_2H product is born with more than 3 eV of internal energy.[16]

In summary, the work presented here demonstrates that the $D + CH_2O(S_0)$ channel is a major pathway in the dissociation of CH_2OD excited to the origin band of the $^2A''(3p_z)$ Rydberg state. Isomerization to the methoxy isomer is not an important pathway. The mechanism involves predissociation, and the dissociation lifetime is on the order of a picosecond. The final dissociation step possibly involves fast, direct cleavage of the O−D bond, and it is the exit-channel dynamics that gives rise to a formaldehyde product with a high degree of internal excitation. The direct sequence of nonradiative pathways is presently unknown, but because channel Ia correlates only with the ground state of hydroxymethyl, coupling to this surface must be the last step in the dissociation sequence. Calculations that take into account both Rydberg and valence states, as well as Rydberg−valence configuration mixing and locations of surface crossings are necessary in order to sort out the mechanisms.

The hydroxymethyl radical can exhibit rich photochemistry both on the ground and the excited potential energy surfaces. For example, additional product channels such as $CH_2 + OH$ are likely to be important for some states, and isomerization may depend on the initial excitation as well. Work currently in progress in our laboratory examines the dependence of the D atom translational energy distributions on the $3p_z$ vibronic level, as well as the appearance of other product channels, and will be reported elsewhere.

Acknowledgment. Support by the U.S. Department of Energy, Office of Basic Energy Sciences, Division of Chemical Sciences is gratefully acknowledged. The authors thank O. Khodykin for helpful discussions and Peter Nishimura for his work on the tripling cell.

References and Notes

(1) Johnson, R. D.; Hudgens, J. W. *J. Phys. Chem.* **1996**, *100*, 19874.
(2) Adams, G. F.; Bartlett, R. J.; Purvis, G. D. *Chem. Phys. Lett.* **1982**, *87*, 311.
(3) Saebø, S.; Radom, L.; Schaefer, H. F. *J. Chem. Phys.* **1983**, *78*, 845.
(4) Aristov, V.; Conroy, D.; Reisler, H. *Chem. Phys. Lett.* **2000**, *318*, 393.
(5) Dóbé, S.; Bérces, T.; Turányi, T.; Márta, F.; Grussdorf, J.; Temps, F.; Wagner, H. G. *J. Phys. Chem.* **1996**, *100*, 19864.
(6) Dulcey, C. S.; Hudgens, J. W. *J. Chem. Phys.* **1986**, *84*, 5262.
(7) Bomse, D. S.; Dougal, S.; Woodin, R. L. *J. Phys. Chem.* **1986**, *90*, 2640.
(8) Cui, Q.; Morokuma, K. *Chem. Phys. Lett.* **1996**, *263*, 54.
(9) Osborn, D. L.; Leahy, D. J.; Neumark, D. M. *J. Phys. Chem.* **1997**, *101*, 6583.
(10) Suits, A., personal communication.
(11) Mahon, R.; McIlrath, T. J.; Myerscough, V. P.; Koopman, D. W. *IEEE J. Quantum Electron.* **1979**, *QE−15*, 444.
(12) Wiley, W. C.; McLaren, I. H. *Rev. Sci. Instrum.* **1955**, *26*, 1150.
(13) Moore, C. E. *Atomic Energy Levels as Derived From the Analyses of Optical Spectra*; National Bureau of Standards (United States): Washington, DC, 1971; Vol. 1.
(14) Callaghan, R.; Arepelli, S.; Gordon, R. J. *J. Chem. Phys.* **1987**, *86*, 5273.
(15) Syage, J. A. *J. Chem. Phys.* **1996**, *105*, 1007.
(16) Wang, J.-H.; Hsu, Y.-T.; Liu, K. *J. Phys. Chem. A* **1997**, *101*, 6593.
(17) Yang, S.-c.; Bersohn, R. *J. Chem. Phys.* **1974**, *61*, 4400.
(18) Chase, M. W.; Davies, C. A.; Downey, J. R.; Frurip, D. J.; McDonald, R. A.; Syverud, A. N. *J. Phys. Chem. Ref. Data* **1985**, *14*.
(19) Walch, S. P. *J. Chem. Phys.* **1993**, *98*, 3163.
(20) Herzberg, G. *Molecular Spectra and Molecular Structure III. Electronic Spectra and Electronic Structure of Polyatomic Molecules*; Van Nostrand Reinhold Company: New York, 1966; Vol. 3.
(21) ΔH_f (CH_2OD) estimated from ΔH_f (CH_2OH) − ZPE (CH_2OH) + ZPE (CH_2OD) from ref 1.
(22) The energetics of channel III was computed for HCOH in ref 19.
(23) Droz-Georget, T.; Zyrianov, M.; Reisler, H.; Chandler, D. W. *Chem. Phys. Lett.* **1997**, *276*, 316.
(24) Rettrup, S.; Pagsberg, P.; Anastasi, C. *Chem. Phys.* **1988**, *122*, 45.
(25) Solgadi, D.; Flament, J. P. *Chem. Phys.* **1985**, *98*, 387.